

Digital Pre-distortion Based on Delta Sigma Modulation Assisted Look-up Table for Optical Transmission

Xiaobo Zeng⁽¹⁾, Mengfan Fu⁽¹⁾, Lilin Yi⁽¹⁾, Weisheng Hu⁽¹⁾, Qunbi Zhuge⁽¹⁾, *

⁽¹⁾ State Key Laboratory of Advanced Optical Communication Systems and Networks, Department of Electronic Engineering, Shanghai Jiao Tong University, Shanghai, 200240, China.

*qunbi.zhuge@sjtu.edu.cn

Abstract A delta-sigma modulation assisted look-up table (LUT) in sample for transceiver nonlinear impairment is proposed, and achieves a superior performance compared with the 3-symbol LUT (LUT-3). The table size is less than 3.2% of the LUT-3 method.

Introduction

With the exponential growth of the traffic within datacenter (DC) [1-3], coherent transceiver is investigated as an promising solution for beyond Tb/s intra-DC interconnection [4-5]. Reduction of cost is essential for the adoption of coherent technology within DC. For high-speed transmission, a coherent transceiver with a high symbol rate and spectral efficiency is more vulnerable to the impairments of low-cost transceiver components [6-7]. At the transmitter (Tx) side, the main impairments include bandwidth limitation and component nonlinearities. To mitigate the nonlinearity and expand the overall linear range of electronic and opto-electronic devices, digital pre-distortion (DPD) can be adopted [8]. Methods for DPD have been proposed including Volterra series [9-10], and neural network [11-12]. Compared with them, the LUT based DPD is potentially a more lightweight alternative with similar performance [13-15]. For the LUT method with the signal dictionary size, D , and memory depth, M , the table size is D^M [16]. The size can be prohibitively large for high-order modulation formats, such as 64- or 256-ary quadrature amplitude modulation (QAM). Methods are proposed to reduce the size by only considering the symbols with high pattern error or high amplitude in the LUT at the cost of performance degradation [17-18]. In addition, aforementioned LUT methods are applied to symbols, depending on the modulation format of signal. For high-speed transmission, the DPD to samples at the input of digital-to-analog converter (DAC) is essential, especially for the systems with sophisticated digital signal processing (DSP) at transmitter.

In this work, we propose a DPD scheme based on delta sigma modulation [19] assisted LUT (DSM-LUT) for samples before DAC. We compare its performance with the 3-symbol LUT (LUT-3) based DPD, and the directly quantized 1-sample LUT (Qtz-LUT-1) based DPD in simulation. The superior performance in terms of

sensitivity is quantified for different nonlinear responses of Tx. The table size is less than 3.2% of the LUT-3 method.

Principle

For the sample data after DSP, the number of amplitude levels is too large to be directly applied for the LUT operation. A direct solution is to quantify the samples for the LUT. The correction terms trained by the quantified samples are added to the transmitted samples. The number of bits of the quantizer should be sufficient to ensure the performance. The dictionary size of the LUT is 2^N with an N -bit quantizer.

In order to reduce the requirement of the number of bits, and simultaneously alleviate the performance degradation caused by quantization, we propose to use the DSM [19] function to convert high-resolution samples to low-resolution samples for the LUT operation:

$$X_{DSM} = DSM(X, n_1, n_2) \quad (1)$$

where X_{DSM} is the DSM counterpart of samples of X . n_1 is the over-sampling-ratio of DSM. n_2 is the number of bits of the quantizer in DSM. For the first order DSM, the example spectrum and waveform of the original and DSM samples are illustrated in Fig. 1. Due to the noise shaping of DSM, n_2 is less than N of the aforementioned direct quantization for the same performance. Note that the table size is reduced with the DSM at the cost of increasing the number of times to look up the correction table.

In the DSM-LUT based DPD, the correction

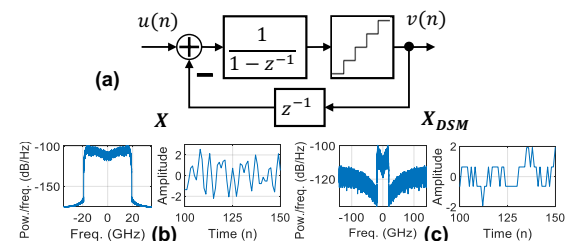


Fig. 1: (a) The first order DSM with a 2-bit quantizer, and an over sampling ratio of 4. The example spectra and waveforms (b) before, and (c) after the DSM.

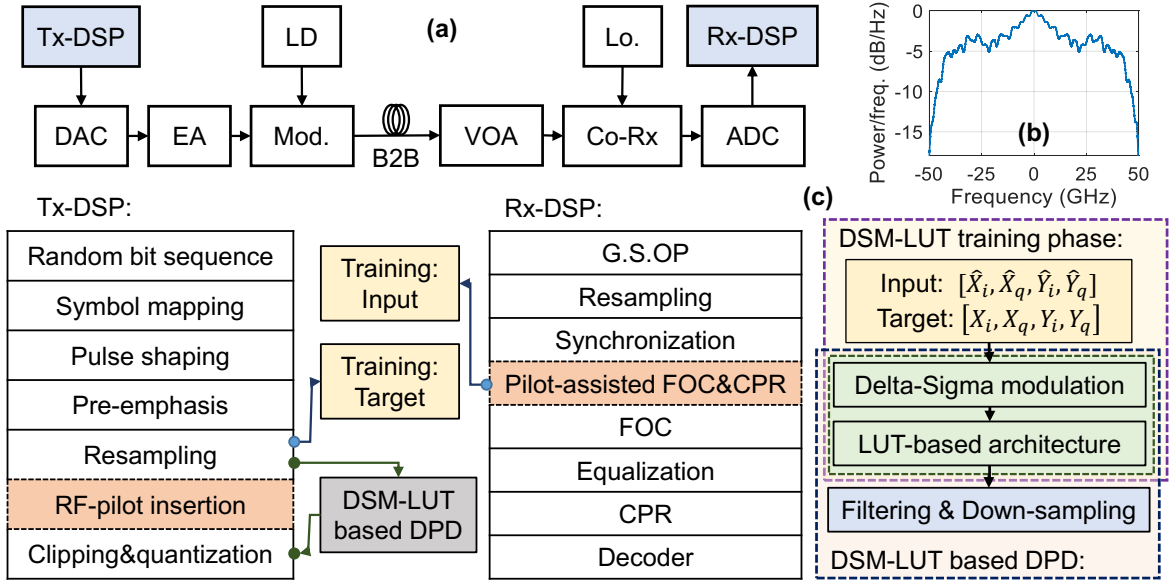


Fig. 2: (a) Simulation setup. (b) Frequency response measured from our experimental setup. (c) Block diagram of the implementation of the DSM-LUT method. LD: laser diode. RF: radio frequency. G.S. OP: Gram-Schmidt orthogonalization procedure. FOC: frequency offset correction. CPR: carrier phase recovery.

table trained by the DSM samples is used. The transmitted samples are firstly converted into the DSM samples as (1). Then, the correction terms stored in the table are obtained based on the neighboring DSM sample pattern, and added into the corresponding samples. A decimator consisted of filtering and down-sampling is used to obtain the pre-distorted signal, as shown in Fig. 2(c).

Simulation setup

The simulation setup is shown in Fig. 2(a), where the Tx- and Rx-digital signal processing (DSP) are described. The blocks of “RF-pilot insertion”, and “Pilot-assisted FOC & CPR” are only used in the training phase of the DSM-LUT method.

In the simulation, a random bit sequence (RBS) is generated by the random function of MATLAB. Then it is mapped into the symbols with the format of 64QAM, and the symbol sequence length is 2^{16} . The root-raised-cosine filter with a roll-off factor of 0.1 is used to shape the signal with a symbol rate of 35Gbaud. The DAC and analog-to-digital converter (ADC) are modeled as the ideal quantizers with the effective number of bits (ENOB) of 6 [20]. The clipping ratio is optimized. The used frequency response of transmitter is shown in Fig. 2(b), which is measured from an experimental setup. For the electric amplifier (EA), the nonlinear response is modelled using the Rapp model of solid-state power amplifier (SSPA) as [11, 21]

$$v_{out} = v_{in} / \sqrt[4]{1 + (v_{in}/V_{sat})^4} \quad (2)$$

where v_{in} , v_{out} , and V_{sat} are the input, output, and the saturation voltage of the EA. The nonlinearity of EA can be adjusted by the back-

off (BO) expressed as [11, 21]

$$BO \text{ [dB]} = 20 \cdot \log_{10}(v_{rms}/V_{sat}) \quad (3)$$

where v_{rms} is the root mean square voltage of the input voltage. The amplified signals are modulated into the carrier by a dual polarization inphase-quadrature Mach-Zehnder modulator. At the receiver side, a variable optical attenuator (VOA) is used to adjust the received optical power (ROP) of signal. The signal is detected by a coherent receiver. Then, the ADCs and Rx-DSP are used to recover the signal. An optical back-to-back (B2B) transmission is considered.

In addition, the “RF-pilot insertion”, and “Pilot-assisted FOC & CPR” are only adopted in the training phase to compensate the carrier phase and frequency offset. In order to eliminate the timing difference, the samples from the Tx and Rx sides, respectively, should be synchronized before the DSM of (1). In order to simplify the DSM function, the first order DSM is used in this work, as shown in Fig. 1(a). The clipping ratios of the quantizer in the DSM are optimized for different over-sampling ratios.

Simulation results and discussions

In order to investigate different scenarios with weak, mild and strong nonlinearity, the BOs are altered to 9 dB, 6 dB, and 3 dB, respectively. For comparison, the proposed DSM-LUT method, the traditional 3-symbol LUT (LUT-3) [13], and the directly quantized LUT (Qtz-LUT) with multi-bit quantizer are evaluated. The DSM-LUT method has the parameter pair of (over sampling ratio of DSM, number of bits of the quantizer), while the Qtz-LUT method has the parameter of number of bits. In this work, due to the memoryless Rapp

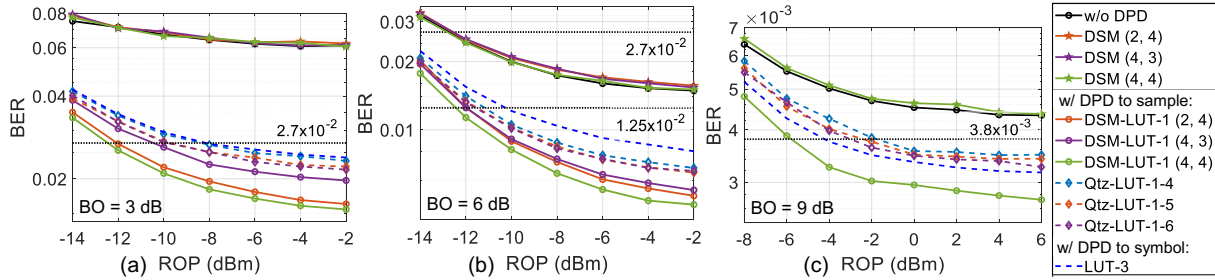


Fig. 3: BER versus received optical power for the different nonlinear scenarios of (a) BO=3 dB, (b) BO=6 dB, and (c) BO=9 dB.

model of SSPA, the memory depths of 1 is applied to the DSM-LUT and Qtz-LUT (i.e., DSM-LUT-1, Qtz-LUT-1). In addition, the soft-decision (SD), concatenated (C) [22] and hard-decision (HD)-forward error correction (FEC) are used with the overhead (OH) of 20%, 14.8% and 7%, respectively. The corresponding BER thresholds are 2.7×10^{-2} , 1.25×10^{-2} , and 3.8×10^{-3} , respectively.

Fig. 3 shows the results for the nonlinearity scenarios of BO = 3 dB, 6 dB, and 9 dB. The performance of the LUT-3 method is used as the benchmark. In order to eliminate the side effect of DSM, the parameters are optimized. The system performance of BER is basically consistent with or without the DSM function, as shown in Fig. 3. Then, DSM-LUT-1 based DPD with the optimized parameters is applied to the systems. In order to present the results concisely, the sensitivity gains in dB versus LUT-3 method are listed in the Tab. 1. We can find that when the Tx is in the scenario with strong nonlinearity (i.e., BO=3 dB), the proposed DSM-LUT-1 method achieves the gains of 3.91 dB, 2.28 dB, and 4.26 dB for the parameter pairs of (2, 4), (4, 3), and (4, 4), respectively, at the SD-FEC. In the scenario with mild nonlinearity (i.e., BO=6 dB), the proposed DPD method obtains the gains of 1.74 dB, 1.75 dB, and 2.13 dB for the parameter pairs of (2, 4), (4, 3), and (4, 4), respectively, at the C-FEC. For the scenario with weak nonlinearity (i.e., BO=9 dB), the proposed DPD method achieves the gains of 1.56 dB for the parameter pairs of (4, 4), at the HD-FEC.

Noted that when the number of bits of the quantizer and the over sampling ratio of DSM are too small, such as (2, 1), (2, 2), (2, 3), (4, 1), and (4, 2), the DSM will degrade the performance due to quantization noise. In addition, compared with the Qtz-LUT-1 method with 4, 5, and 6 bits, the proposed DPD achieves better sensitivities due to the effect of DSM of (1) with the optimized parameters, as shown in Tab. 1. When the number of bits of the quantizer is too small, such as, 1, 2, and 3, the quantization noise leads divergency to the correction terms of LUT, and degrades the performance of Qtz-LUT-1 method.

Tab. 1: Sensitivity gains of the DSM-LUT-1 and Qtz-LUT-1 based DPD versus the LUT-3 method.

Sensitivity gain (dB / vs. LUT-3)	BO=3dB	BO=6dB	BO=9dB	LUT size	
FEC type	20% OH SD-FEC	14.8% OH C-FEC	7% OH HD-FEC		
LUT-3	Benchmark			512	
Qtz - LUT - 1	4	0.19	0.87	16	
	5	1.54	1.22	32	
	6	1.70	1.30	64	
DSM-LUT - 1	(2, 4)	3.91	1.74	16	
	(4, 3)	2.28	1.75	8	
	(4, 4)	4.26	2.13	1.56	16

Note that the table size is reduced with the DSM. The table size of the DSM-LUT-1 is less than or equal to 16, which is less than 3.2% of the size of LUT-3 based method.

Conclusions

In this work, we propose a DPD scheme for samples based on the DSM assisted LUT. Extensive simulations are conducted based on the Rapp model of SSPA. Compared with the LUT-3 and the Qtz-LUT-1 methods, the proposed DPD achieves the gains of sensitivity up to 4.26 dB, 2.13 dB, and 1.56 dB for the nonlinear scenarios with the BOs of 3 dB, 6dB, and 9 dB at the BER threshold of 2.7×10^{-2} , 1.25×10^{-2} , and 3.8×10^{-3} , respectively. The table size is less than 3.2% of the size of LUT-3 method.

Acknowledgements

This work was supported by National Key R&D Program of China (2018YFB1801200), and NSFC (62175145).

References

- [1] K. Zhong, X. Zhou, J. Huo, C. Yu, C. Lu, and A. P. T. Lau, "Digital signal processing for short-reach optical communications: a review of current technologies and future trends," *J. Lightwave Technol.*, vol. 36, no. 2, pp. 377–400, Jan. 2018, doi: 10.1109/JLT.2018.2793881.
- [2] "Cisco annual internet report (2018–2023).pdf." [Online].

- Available: <https://www.cisco.com/c/en/us/solutions/collateral/executive-perspectives/annual-internet-report/white-paper-c11-741490.html>
- [3] S. Kumar, G. Papen, K. Schmidtke, and C. Xie, "Intra-data center interconnects, networking, and architectures," in *Optical Fiber Telecommunications VII*, Elsevier, 2020, pp. 627–672. doi: 10.1016/B978-0-12-816502-7.00016-6.
- [4] J. Cheng, C. Xie, Y. Chen, X. Chen, M. Tang, and S. Fu, "Comparison of coherent and IMDD transceivers for intra datacenter optical interconnects," in *Optical Fiber Communication Conference (OFC) 2019*, San Diego, California, 2019, p. W1F.2. doi: 10.1364/OFC.2019.W1F.2.
- [5] X. Zhou, R. Urata, and H. Liu, "Beyond 1 Tb/s intra-data center interconnect technology: IM-DD or coherent?," *J. Lightwave Technol.*, vol. 38, no. 2, pp. 475–484, Jan. 2020, doi: 10.1109/JLT.2019.2956779.
- [6] D. Sadot, Y. Yoffe, H. Faig, E. Wohlgemuth, "Digital pre-compensation techniques enabling cost-effective high-order modulation formats transmission," *J. Lightwave Technol.*, vol. 37, no. 2, p. 10, 2019. doi: 10.1109/JLT.2018.2888941.
- [7] E. de Souza Rosa, J. Helio Da Cruz, and T. Sutili, "Digital pre-distortion employing complex FIR filters from receiver side two stage dynamic equalizer for coherent optical systems," in *2021 SBMO/IEEE MTT-S International Microwave and Optoelectronics Conference (IMOC)*, Fortaleza, Brazil, Oct. 2021, pp. 1–3. doi: 10.1109/IMOC53012.2021.9624890.
- [8] Q. Zhou *et al.*, "Digital predistortion enhancement by convolutional neural network for probabilistic shaped discrete multi-tone signal transmission in passive optical network," in *Optical Fiber Communication Conference (OFC) 2021*, Washington, DC, 2021, p. M3G.3. doi: 10.1364/OFC.2021.M3G.3.
- [9] Lei Guan and Anding Zhu, "Low-cost FPGA implementation of Volterra series-based digital predistorter for RF power amplifiers," *IEEE Trans. Microwave Theory Techn.*, vol. 58, no. 4, pp. 866–872, Apr. 2010, doi: 10.1109/TMTT.2010.2041588.
- [10] D. R. Morgan, Z. Ma, J. Kim, M. G. Zierdt, and J. Pastalan, "A generalized memory polynomial model for digital predistortion of RF power amplifiers," *IEEE Trans. Signal Process.*, vol. 54, no. 10, pp. 3852–3860, Oct. 2006, doi: 10.1109/TSP.2006.879264.
- [11] G. Paryanti, H. Faig, L. Rokach, and D. Sadot, "A direct learning approach for neural network based pre-distortion for coherent nonlinear optical transmitter," *J. Lightwave Technol.*, vol. 38, no. 15, pp. 3883–3896, Aug. 2020, doi: 10.1109/JLT.2020.2983229.
- [12] Y. Wu, U. Gustavsson, A. G. i Amat, and H. Wymeersch, "Residual neural networks for digital predistortion," in *GLOBECOM 2020 - 2020 IEEE Global Communications Conference*, Taipei, Taiwan, Dec. 2020, pp. 01–06. doi: 10.1109/GLOBECOM42002.2020.9322327.
- [13] J. H. Ke, Y. Gao, and J. C. Cartledge, "400 Gbit/s single-carrier and 1 Tbit/s three-carrier superchannel signals using dual polarization 16-QAM with look-up table correction and optical pulse shaping," *Opt. Express*, vol. 22, no. 1, p. 71, Jan. 2014, doi: 10.1364/OE.22.000071.
- [14] Z. He, K. Vijayan, M. Mazur, M. Karlsson, and J. Schroder, "Look-up table based pre-distortion for transmitters employing high-spectral-efficiency modulation formats," in *2020 European Conference on Optical Communications (ECOC)*, Brussels, Belgium, Dec. 2020, pp. 1–4. doi: 10.1109/ECOC48923.2020.9333231.
- [15] D. Byrne, R. Farrell, and J. Dooley, "Recursive pre-distorter for hardware efficient digital pre-distortion," in *2021 IEEE Topical Conference on RF/Microwave Power Amplifiers for Radio and Wireless Applications (PAWR)*, San Diego, CA, USA, Jan. 2021, pp. 31–33. doi: 10.1109/PAWR51852.2021.9375537.
- [16] H. Faig, B. V. Pedersen, S. Cohen, L. Gantz, and D. Sadot, "Nonlinear system identification scheme for efficient compensators design," *J. Lightwave Technol.*, vol. 38, no. 13, pp. 3519–3525, Jul. 2020, doi: 10.1109/JLT.2019.2963252.
- [17] J. Zhang *et al.*, "PAM-8 IM/DD transmission based on modified lookup table nonlinear predistortion," *IEEE Photonics J.*, vol. 10, no. 3, pp. 1–9, Jun. 2018, doi: 10.1109/JPHOT.2018.2828869.
- [18] S. Zhalehpour, J. Lin, W. Shi, and L. A. Rusch, "Reduced-size lookup tables enabling higher-order QAM with all-silicon IQ modulators," *Opt. Express*, vol. 27, no. 17, p. 24243, Aug. 2019, doi: 10.1364/OE.27.024243.
- [19] S. Pavan, R. Schreier, G. C. Temes, and R. Schreier, *Understanding delta-sigma data converters*, Second edition. Hoboken, New Jersey: IEEE Press/Wiley, 2017.
- [20] O. Funke, "M8194A 120 GSa/s arbitrary waveform generator," p. 8.
- [21] V. Bajaj, M. Chagnon, S. Wahls, and V. Aref, "Efficient training of Volterra series-based pre-distortion filter using neural networks," in *Optical Fiber Communication Conference (OFC)*, 2022, San Diego, California, p. 3.
- [22] "Implementation agreement 400ZR," 2020. [Online]. Available: https://www.oiforum.com/wp-content/uploads/OIF-400ZR-01.0_reduced2.pdf